

## COGNITIVE NEUROSCIENCE

# The representation of Kanizsa illusory contours in the monkey inferior temporal cortex

Gy. Sáry, K. Köteles, P. Kaposvári, L. Lenti, G. Csifcsák, E. Frankó, G. Benedek and T. Tompa  
Department of Physiology, Faculty of Medicine, University of Szeged, H-6720, Szeged, Dóm tér 10. Hungary

**Keywords:** illusory contour, inferior temporal cortex, Kanizsa figures, rhesus monkey, shape selectivity

## Abstract

Stimulus reduction is an effective way to study visual performance. Cues such as surface characteristics, colour and inner lines can be removed from stimuli, revealing how the change affects recognition and neural processing. An extreme reduction is the removal of the very stimulus, defining it with illusory lines. Perceived boundaries without physical differences between shape and background are called illusory (or subjective) contours. Illusory and real contours activate early stages of the macaque visual pathway in similar ways. However, data relating to the processing of illusory contours in higher visual areas are scarce. We recently reported how illusory contours based on abutting-line gratings affect neurones in the monkey inferotemporal cortex, an area essential for object and shape vision. We now present data on how inferotemporal cortical neurones of monkeys react to another type of shapes, the Kanizsa figures. A set of line drawings, silhouettes, their illusory contour-based counterparts, and control shapes have been presented to awake, fixating rhesus monkeys while single-cell activity was recorded in the anterior part of the inferotemporal cortex. Most of the recorded neurones were responsive and selective to shapes presented as illusory contours. Shape selectivity was proved to be different for line drawings and illusory contours, and also for silhouettes and illusory contours. Neuronal response latencies for Kanizsa figures were significantly longer than those for line drawings and silhouettes. These results reveal differences in processing for Kanizsa figures and shapes having real contours in the monkey inferotemporal cortex.

## Introduction

Trying to find the principles of visual processing in the inferior temporal (IT) cortex, researchers have used stimulus-reduction to find the features determining the responses of IT cells (Tanaka, 1992; Sugase *et al.*, 1999). In earlier studies we systematically removed the surface-determining features of complex, coloured stimuli. We removed the colour (Tompa *et al.*, 2005), shading, texture, internal contours, and all the contours, leaving only the luminance-defined silhouette of the stimuli (Kovacs *et al.*, 2003). In the present study we removed the whole stimulus, representing it with physically non-existent illusory contours, defined by Kanizsa-type inducers. Our question was, how do the neurones' responses change (individually and at the population level) if the stimulus they have been selectively responding to is present only in an induced form.

A fruitful method for investigating sensory systems is to study the instances in which they are deceived. Objects can generally be visually separated from the background only if they differ in physical parameters (colour, texture, luminance etc.). Illusory contours (ICs) are subjectively perceived boundaries without such differences

(Ramachandran, 1987), so they can reveal mechanisms of perceptual organization, e.g. mechanisms of figure-ground segregation, border ownership assignment, perceptual grouping and contour integration (Gilbert & Sigman, 2007).

The perception of illusory contours has been widely studied. Findings suggest that the processing of real contours and ICs are subject to similar cortical mechanisms (von der Heydt *et al.*, 1984; Vogels & Orban, 1987). Real contours and ICs activate early stages of the monkey visual pathway (Peterhans & von der Heydt, 1991; Grosf *et al.*, 1993; Sheth *et al.*, 1996; Lee & Nguyen, 2001), but in area 17 ICs seem to trigger activity differing from that elicited by real contours (Ramsden *et al.*, 2001). The results of psychophysical and imaging studies support the importance of early areas in the processing of ICs (Pillow & Rubin, 2002; Maertens & Pollmann, 2005); at the same time, imaging studies unanimously suggest the contribution of a wide network of visual areas including higher order ones (Larsson *et al.*, 1999; Montaser-Kouhsari *et al.*, 2007). Interestingly, cellular level data is missing for IC computation in higher areas (Montaser-Kouhsari *et al.*, 2007).

The IT cortex is an area believed to be essential for shape and object vision (Dean, 1976) and the properties of the IT cortical neurones parallel the invariances of object perception in many aspects (Rolls & Baylis, 1986; Hasselmo *et al.*, 1989; Tovee *et al.*, 1994; Logothetis *et al.*, 1995; Logothetis & Sheinberg, 1996; Tanaka, 1996; Wallis &

Correspondence: Dr G. Benedek, as above.  
E-mail: benedek@phys.szote.u-szeged.hu

Received 15 May 2008, revised 19 August 2008, accepted 10 September 2008

Rolls, 1997; Booth & Rolls, 1998). The role of the IT cortex in IC processing is not clear. Some studies suggest that the discrimination of IC shapes is disrupted after lesions of the IT (Merigan, 1996; Huxlin *et al.*, 2000). We recently described how cells react to ICs based on abutting-line gratings (Vogels & Orban, 1987) in the monkey IT cortex (Sary *et al.*, 2007). In the present study we tested whether IT cortical neurones respond to shapes defined by the Kanizsa type (Kanizsa, 1976) ICs (KICs).

## Materials and methods

### Subjects and surgery

Two adult macaque monkeys (C and H, weighing 7.3 and 6.5 kg, respectively, at the time of the experiments) were used as subjects. Both animals received a stainless steel headpost to allow the fixation of the head during the training and recording sessions. A recording chamber (Narishige, Tokyo, Japan) was fixed to the skull and a scleral search coil was implanted into one eye (Judge *et al.*, 1980) to monitor eye movements. Before surgery, an MRI image was obtained from the brain of each monkey. The images and a stereotaxic atlas of the monkey brain (Paxinos *et al.*, 1999) were used to find coordinates for the recording chamber. The surgical procedures were performed under general anaesthesia and under aseptic conditions. Anaesthesia was induced with Calypsol (ketamine; 20 mg/kg i.m.) and maintained with 1.5% halothane in a 2 : 1 mixture of N<sub>2</sub>O and O<sub>2</sub>. Atropine (0.05 mg/kg i.m.) was injected to reduce bronchial secretion and salivation. Body temperature, heart rate, respiratory rate, end-tidal CO<sub>2</sub> and peripheral O<sub>2</sub> saturation were monitored throughout the surgery. Analgesic was given after surgery (Nalbuphine, 0.15 mg/kg) for 5 days.

We used a controlled water-access paradigm during the training of the animals and for the recording sessions. Monkey C was killed with an overdose of nembutal and perfused with fixative at the end of the experiments. Recording sites could be reconstructed by identifying the tracks of the last few penetrations (see fig. 2 in Sary *et al.*, 2004). Monkey H is still participating in experiments. Penetration locations in this animal were confirmed by the transitions of grey and white matter activity during recording sessions, by the depth of electrode tract reaching the bone, by the shape-selectivity of the recorded cells and by the response onset latency values. All procedures were approved by the Ethical Committee for Animal Experiments at the University of Szeged and conformed to the guidelines of the NIH for the care and use of laboratory animals.

### Apparatus and stimuli

Standard electrophysiological equipment (FHC Inc., Bowdoin, ME, USA) and tungsten microelectrodes (impedance ~3 M $\Omega$ ; FHC) were used to record single-cell activity from the IT cortex. Signals were amplified, bandpass-filtered (FHC; 500–2000 Hz) and fed into a window-discriminator, and the timing of the spikes was stored on disk with a sampling rate of 1 kHz. Eye movements were recorded via a search coil system (DNI Instruments, Newark, DE, USA) with a sampling rate of 250 Hz. Custom-made software controlled the experiment: it recorded eye movements, delivered the reward (fruit juice and water), monitored the animals' behaviour and controlled the stimulus presentation and the collection of electrophysiological data.

All stimuli were presented on a uniform white background (square width: 18°, luminance 23 cd/m<sup>2</sup>). A set of 20 nonchromatic stimuli, line drawings (LDs), composed of a combination of Kanizsa inducers and line contours, were used to isolate the cells (Fig. 1A). The LD

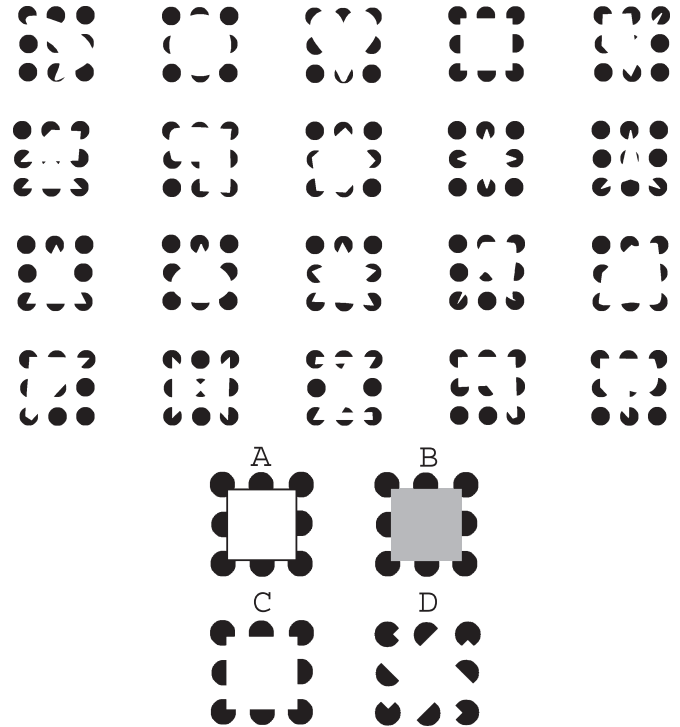


FIG. 1. Upper part, the set of Kanizsa stimuli used in the present study; lower part, example of the modifications of the stimuli: a square represented as (A) a line drawing (LD), (B) a silhouette (SIL), (C) a Kanizsa figure (KIC) and (D) control (CTR).

stimuli themselves had a square width of 14° and the mean luminance of the whole stimulus was 19 cd/m<sup>2</sup> as seen by the monkeys. Silhouettes (SILs) were made by filling up the area between the 'pacmen' (the inducers) with a homogeneous grey (luminance 1.5 cd/m<sup>2</sup>; Fig. 1B). The mean luminance of the SILs was 16 cd/m<sup>2</sup>. KICs were produced by removing the black lines from the LDs (Fig. 1, upper part and panel C). In this way we generated perceived edges between the pacmen producing different KICs (mean luminance 20 cd/m<sup>2</sup> as seen by the monkeys). Control stimuli (CTRs) were made by using the pacmen of the KICs: the pacmen were rotated out of their original position (see e.g. Brodeur *et al.*, 2006), thereby no longer producing KICs whilst retaining the geometrical details of the inducers (Fig. 1D). The mean luminance of the CTRs from the monkeys' position was 20 cd/m<sup>2</sup>.

Stimuli were presented on a display [Philips Brilliance 17A (4CM6282/20T)], with 17' diameter (~16' viewable). Refresh rate, resolution of the screen and viewing distance were 74 Hz, 800 × 600 pixels and 57 cm, respectively.

### Stimulus sequence and single-cell recording protocol

Animals were trained using operant conditioning and a controlled water-access paradigm. A fixation task was used during the recording sessions. The animals were seated in a primate chair in a dark room, with their head fixed. A trial started with the onset of a blue fixation spot (arc diameter, 6 min; luminance, 5.5 cd/m<sup>2</sup>) on a dark background on the computer screen. The animal had 500 ms to start the fixation (fixation window, 0.5 × 0.5°); delay resulted in an abort. If the animal started to fixate, first a white background was presented. After 300 ms, nine black discs (the inducers without the notches) appeared for 400 ms, followed by the stimuli themselves for 500 ms.

The fixation spot remained on the screen for a further 100–300 ms after the end of the stimulus and drops of fruit juice or water were given as reward. Single cells were isolated using the LD stimuli by advancing the electrode with a hydraulic microdrive (Narishige). First, every stimulus was presented at least five times in a pseudorandom sequence. The effectiveness of the stimulus (the magnitude of the cellular responses) was estimated upon inspection of the peristimulus time histogram (PSTH) and auditory feedback online. Visual inspection of the PSTH is a common method used to decide the effectiveness of a stimulus before the actual test and the statistical evaluation (DiCarlo & Maunsell, 2000; Tamura & Tanaka, 2001; Kovacs *et al.*, 2003). This selection method was confirmed by offline analysis. Once a cell was found to be responsive to at least one of the stimuli, we tested the cells using six shapes of the original set of 20: three eliciting the largest firing rates from a particular neurone ('effective stimuli') and three which triggered only a moderate response or no response at all ('noneffective stimuli'). (As IT cortical neurons are often selective for stimuli, the effective and noneffective stimuli differed from cell to cell, i.e., each cell was tested with a different set of six stimuli. See also Figs 2 and 3.) Each of the six shapes was then presented under the different stimulus conditions (LDs, KICs, SILs and CTR) in an interleaved fashion, at least 10 times. Breaking fixation during the trial resulted in an abort. Only data from fully finished trials were included in this study.

### Behavioural test

To prove that animals are able to perceive the KICs, one of the monkeys received recognition training. Details were published earlier (Kovacs *et al.*, 2003; Sary *et al.*, 2006), so we only give a brief summary of the method. The twenty LDs were classified in two groups and 10 stimuli were associated with a left-side saccade while the other 10 were associated with a right-side saccade. The end of the LD stimuli was followed by the appearance of two small red target spots on both edges of the screen. On the basis of the training the animal had to decide to which side to make the saccade and correct responses were rewarded with drops of water or fruit juice.

Once the animal reached an average performance of 90% correct with LDs, stimuli were intermixed with SILs and KICs. During these trials the animal was rewarded for the SILs or KICs, regardless of the responses it gave. The equal rewarding for correct and incorrect responses allowed measurement of the recognition performance for the novel SILs and KICs (Vogels, 1999).

### Data analysis

We analysed spike counts offline in two 300-ms time windows. The first window, from –300 to 0 ms (0 was the stimulus onset time) served for estimation of the baseline activity, and the second was used to calculate the stimulus-evoked response (100–400 ms). For data analysis, net responses were used; these were calculated by a trial-wise subtraction of the baseline activity from the spike count during stimulus presentation. A response to a stimulus was defined as a statistically significant change in firing rate relative to the baseline (single-sample *t*-test). To make statistical comparisons between the response levels, we took the responses given to the most effective stimulus in every condition. In this way, the neuronal activities of the cells in response to the best (quasi-optimal) images in the different conditions could be compared.

The response onset latency was calculated by using a modified Poisson spike train analysis (Legendy & Salcman, 1985; Sary *et al.*,

2006). For this analysis, the latency values measured for the first effective stimulus (the one evoking the largest response) were used. For each trial, we took the beginning of the first activation phase after the stimulus onset. This was corrected with a weighted sum of the times of occurrence of the spikes preceding it (but still after stimulus presentation). The reciprocals of the numbers of spikes after the given spike were used as weights.

$$t_{\text{lat}} = t_{\text{burst1}} - \sum_{i=1}^n \frac{t_i}{N-i}$$

where  $t_{\text{lat}}$  is the latency,  $t_{\text{burst1}}$  is the beginning of the first activation,  $t_i$  are the arrival times of spikes between the stimulus onset and  $t_{\text{burst1}}$ ,  $n$  is the number of spikes between the stimulus onset and  $t_{\text{burst1}}$ , and  $N$  is the number of spikes after the stimulus onset.

The latency values for a given cell and stimulus were the trial-wise averages of the values described above. This method provided latencies consistent with the PSTH.

To assess the stimulus selectivity of the cells, tuning curves were constructed in the following way: for each neurone and condition, we first ranked the six selected stimuli according to their absolute net responses in one condition (in this case KIC); thus, a tuning curve for that particular condition was obtained. Next, the same stimulus ranking was used for the stimuli in the other condition(s), and the mean absolute activities evoked by the stimuli in this condition were used to make the tuning curve for that particular condition (Sary *et al.*, 1993, 2007; Kovacs *et al.*, 2003). ANOVA, single-sample *t*-test and the Wilcoxon matched *t*-test were used for statistical evaluation. Tests were classified as significant if the corresponding type I error was  $< 0.05$ .

## Results

### Behavioural test

After the animal had reached a performance of 90% correct with the LDs, SILs and KICs were intermixed with the LDs. In this mixed condition, the performances were (mean  $\pm$  SEM) LDs, 90.05  $\pm$  2.2; SILs, 90.3  $\pm$  2.1; KICs, 86.7  $\pm$  2.8; and CTR, 59.1  $\pm$  4.0 correct. An ANOVA and a *post hoc* test (Fisher) revealed that the performances for LDs, SILs and KICs did not differ, and the animal performed for these conditions much better than for the CTR, for which the performance was slightly above chance (ANOVA,  $F = 26.94$ ,  $P = 0.000$ ).

### Single-cell recording

The responses of 129 cells from the two monkeys tested for LDs, KICs, SILs and CTRs were analysed. There was no difference between the results of the two animals so data were pooled. Of these 129 cells, 99 (80 cells from monkey C and 19 cells from monkey H; altogether 76.7%) were found to be selective for the KICs (ANOVA). The results of this study were derived from these cells. The neurones recorded were located on the lower bank and fundus of the superior temporal sulcus and the lateral convexity of the inferior temporal gyrus, in region TE, at stereotaxic coordinates around anterior 17 (see fig. 2 in Sary *et al.*, 2004).

### Responsiveness and selectivity

Figure 2 depicts the PSTHs of two neurones isolated from the IT cortex. These neurones gave significant responses only to the LDs. The neurones also exhibited selectivity for the stimuli: the cell in the

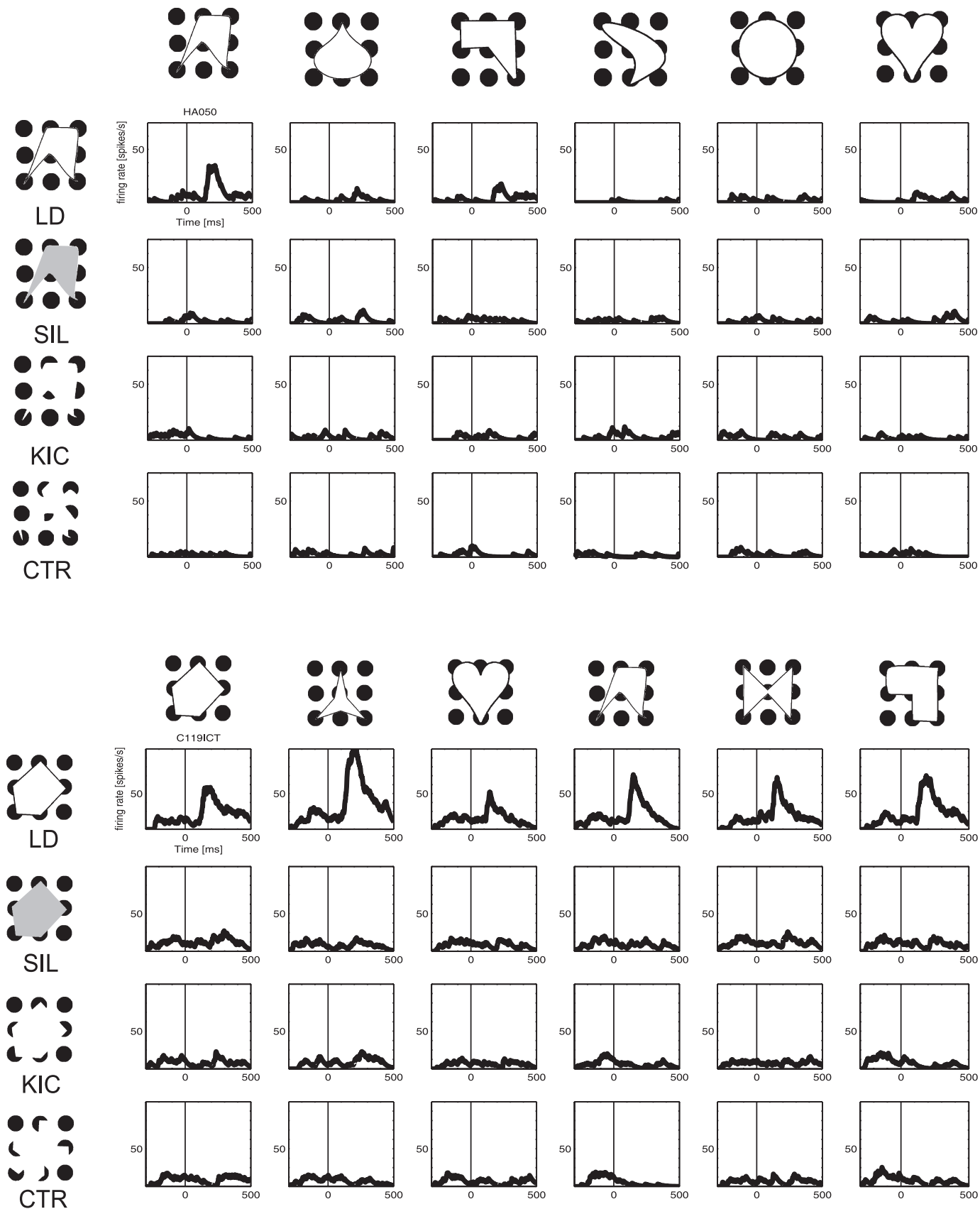


FIG. 2. PSTHs from two IT cells recorded from monkey H (top) and from monkey C (bottom). The set of line drawing stimuli are shown on top of each PSTH. The line at 0 indicates stimulus onset. The upper row shows PSTHs for line drawings (LDs), the second for silhouettes (SILs), the third for illusory contours (KICs) and the last for the controls (CTR).

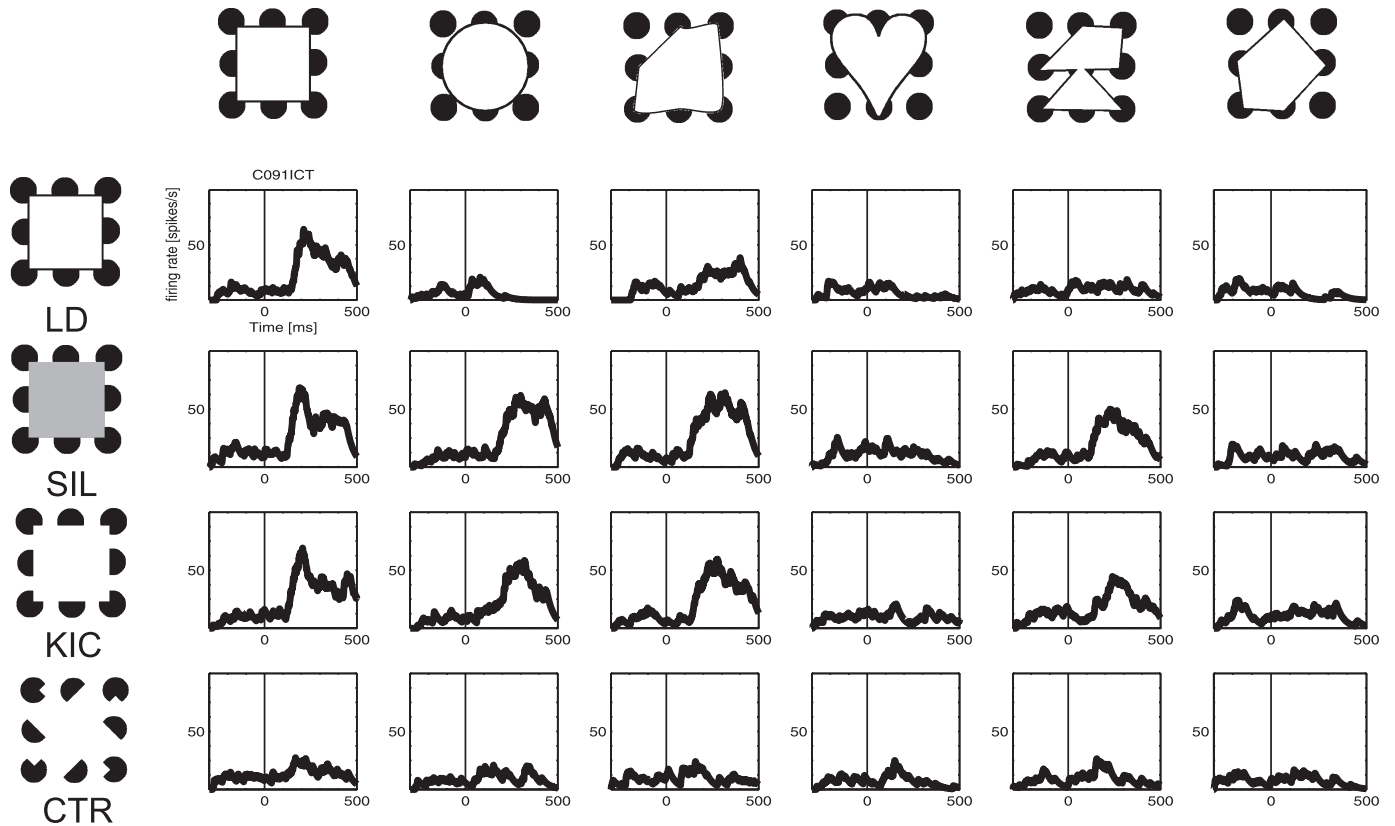


FIG. 3. PSTH from one IT cell recorded from monkey C. The set of line drawing stimuli is shown on top of the PSTH. The conventions are the same as in Fig. 2.

top panel responded only to the first stimulus (ANOVA in the LDs condition,  $F = 3.96$ ,  $P = 0.004$ ), and the responses of the cell in the bottom panel reveal a clear stimulus preference among LDs (first row; ANOVA in the LDs condition,  $F = 9.49$ ,  $P = 0.001$ ). The CTR stimuli did not elicit significant above-background responses.

We first demonstrated that IT cells react to KIC stimuli. Figure 3 shows a single cell responding to LDs, SILs and KICs but not to the CTRs. The cell was shape-selective: with the exception of the CTRs, the responses within a condition differed markedly from each other as estimated with ANOVA (in the LD condition,  $F = 31.54$ ,  $P = 0.001$ ; in the SIL condition,  $F = 32.97$ ,  $P = 0.001$ ; in the KIC condition,  $F = 20.34$ ,  $P = 0.001$ ; in the CTR condition,  $F = 4.71$ ,  $P = 0.1478$ ).

At the population level, the mean  $\pm$  SEM baseline activity was  $11.7 \pm 1.11$  spikes/s and the mean net responses given to the LDs, SILs, KICs and CTRs were  $20.83 \pm 1.80$ ,  $28.10 \pm 2.13$ ,  $24.23 \pm 2.02$  and  $13.31 \pm 1.70$  spikes/s, respectively. For this, we took the best responses in each condition of each cell, thus the responses of the 'optimal' stimulus in every condition could be used. The distribution of the responses in the different conditions can be seen in Fig. 4.

The responses differed significantly between the conditions LD, SIL, KIC and CTR. (ANOVA,  $F = 35.60$ ,  $P = 0.000$ ). A *post hoc* (Fisher) test revealed that the mean response levels to the CTRs were lower than in any other condition. This shows clearly that IT cortical cells react well in the different conditions, including the KICs (Fig. 4). In addition, we found that the responses to the SILs were larger than to the LDs.

We also wanted to establish whether IT cortical cells are capable of responding selectively to KIC stimuli. We found that 76.7% of the recorded neurones were selective for the KIC stimuli presented (ANOVA). Figure 5 illustrates a population tuning curve for these in the

KIC and CTR conditions. The tuning curves in the KIC and CTR conditions differed significantly; the curve for the KICs had a significant slope (ANOVA,  $F = 55.21$ ,  $P = 0.000$ ) while the corresponding plot for the CTR condition ran practically parallel to the x-axis (ANOVA,  $F = 1.05$ ,  $P = 0.383$ ). This indicates shape selectivity for the KICs.

We then compared the shape-selective responses of the IT cortical neurones to the responses evoked by the same stimuli having real contours. We performed the same analysis regarding selectivity for the responses to the KIC, LD and SIL stimuli as described for the KIC and CTR above. Table 1 shows the number of cells having different or similar selectivity in the used conditions and Fig. 6 presents the population-tuning curves obtained under these conditions.

The selectivity in the KIC, LD and SIL conditions differed significantly, the flattest plot being observed for the LDs. The KICs evoked significantly larger responses from the IT cortical cells than did the LDs (Wilcoxon,  $P = 0.001$ ). To exclude the possibility of having tuning curve differences based on markedly different firing rates we repeated the analysis, but with the responses ranked according to the responses to the LDs. The results were similar: as can be seen in Fig. 7, although the tuning curves display a similar course there was a highly significant difference between the tuning curves obtained for the LDs and the KICs ( $F = 17.14$ ,  $P = 0.000$ ).

As the KICs often give the impression of a plane floating above the inducing elements, and the IT cortical cells are sensitive to the inner features of a particular stimulus (Vogels & Biederman, 2002), we tested whether the activity levels evoked by the KICs were similar to those evoked by the SILs of the same shapes. The responses evoked by the SILs were greater than those evoked by the KICs (Wilcoxon,  $P = 0.000$ ), but we found a significant correlation between the

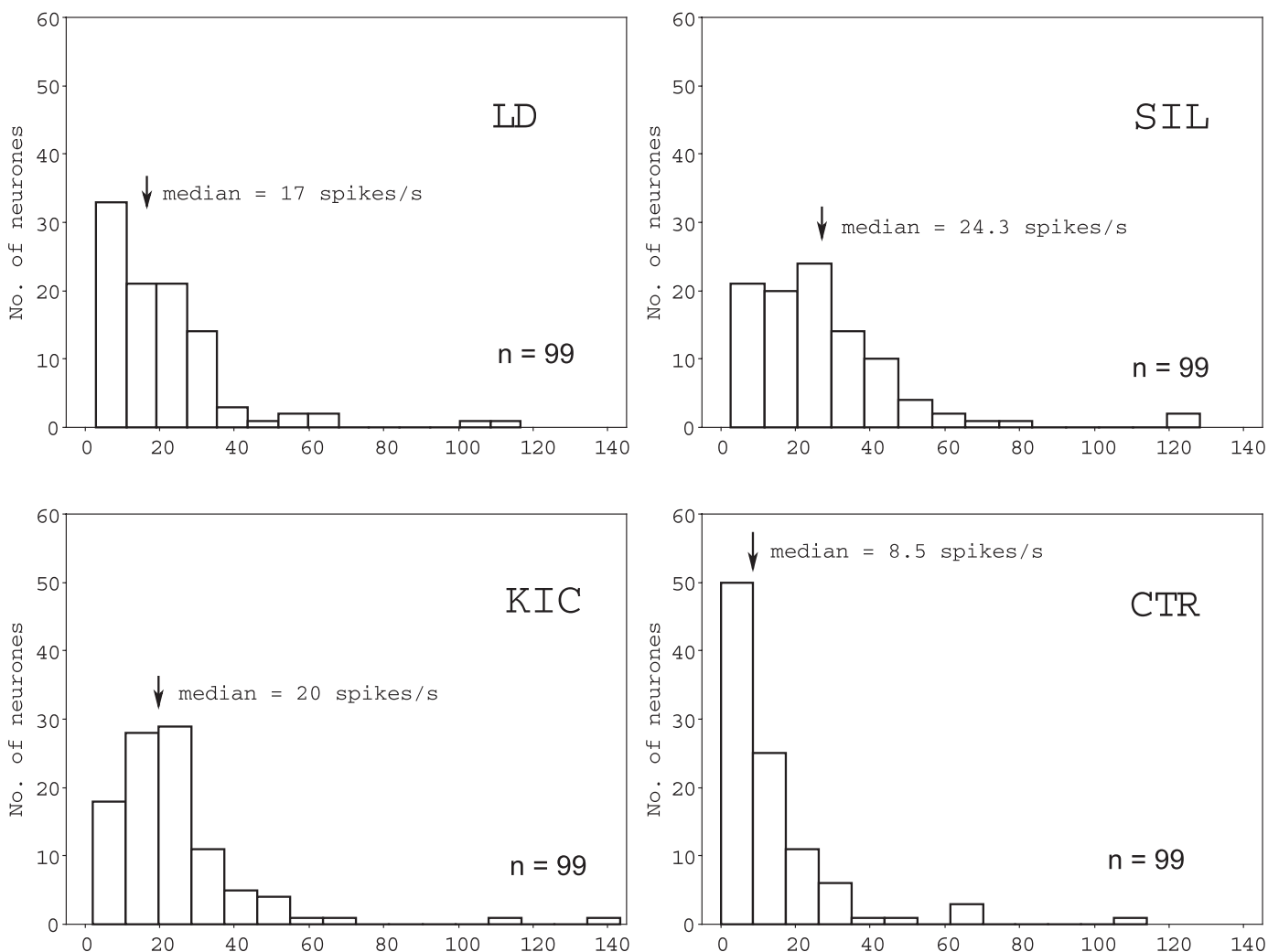


FIG. 4. Distribution of the net responses of IT cortical cells in the LD, SIL, KIC and CTR conditions. The arrows indicate the medians of the distributions.

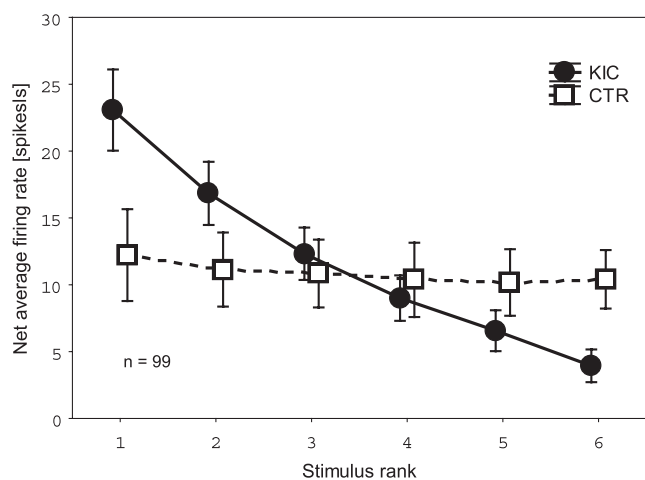


FIG. 5. Tuning curves for the KICs and their CTRs. Means and 0.95 confidence intervals are shown. The line with the full circles shows values for KICs and that with the empty rectangles shows values for CTRs. The ranking was made on the basis of the responses given to the KICs. The two curves differ markedly.

TABLE 1. Numbers of cells having different or similar selectivity

Stimulus	No. neurones	
	Different selectivity	Similar selectivity
LD vs. SIL	79	20
LD vs. KIC	86	13
LD vs. CTR	87	12
SIL vs. KIC	70	29
SIL vs. CTR	83	16
KIC vs. CTR	80	19

CTR, control stimulus; KIC, Kanizsa-type illusory contour; LD, line drawing; SIL, silhouette.

responses given to the SILs and to the KICs (Spearman rank order correlations,  $0.77, P < 0.05$ ). Still, although the slopes of the tuning curves obtained for the KICs and the SILs are more similar to each other than for the KICs and the LDs (Fig. 6), there was a significant difference between the curves (ANOVA,  $F = 20.61, P = 0.000$ ). It is worthwhile noting that the largest ratio of cells having similar selectivity was found in the KIC–SIL comparison (Table 1).

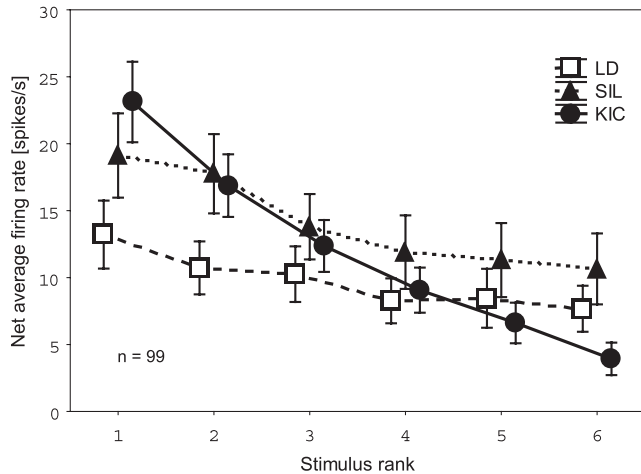


FIG. 6. Tuning curves for the LDs, SILs and KICs. Means and 0.95 confidence intervals are shown. The ranking was made on the basis of the responses given to the KICs. The curves differ significantly.

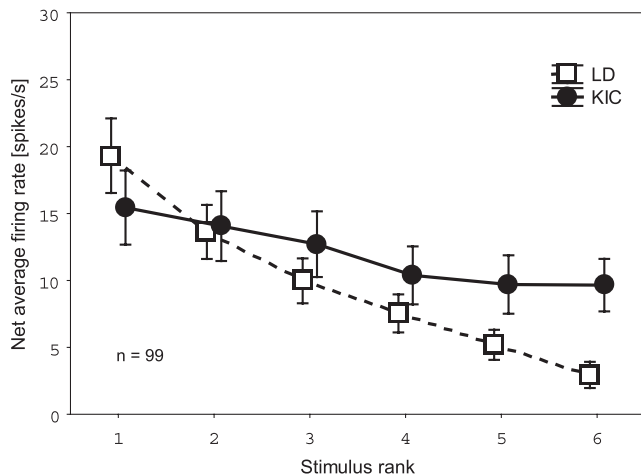


FIG. 7. Tuning curves obtained for the KICs and the LDs. Means and 0.95 confidence intervals are shown. The line with the full circles shows values for the KICs and that with the empty rectangles values for the LDs. The two curves differ significantly. Please note that on this graph the ranking was made on the basis of the responses given to LDs, hence the shape of the curves representing the LDs and KICs differs from those in Fig. 6.

### Response latencies

The latency values obtained by Poisson spike train analysis in the different conditions were  $136.47 \pm 34.96$  ms (mean  $\pm$  SD) for the LDs,  $135.39 \pm 30.33$  ms for the SILs and  $147.99 \pm 36.06$  ms for the KICs. We found significant differences as estimated by ANOVA ( $F = 7.30$ ,  $P = 0.001$ ,  $n = 76$ ); the latency values for the KICs were longer (Fisher *post hoc* test) than those measured in the two other conditions (Fig. 8).

### Discussion

To the best of our knowledge, this is the first single-cell recording study using KIC stimuli in the IT cortex of primates. We presented shapes having real contours (LDs and SILs) and KICs to fixating monkeys while recording the neuronal activity in the IT cortex, and compared the responses to KICs and real contours. Our main findings can be summarized as follows:

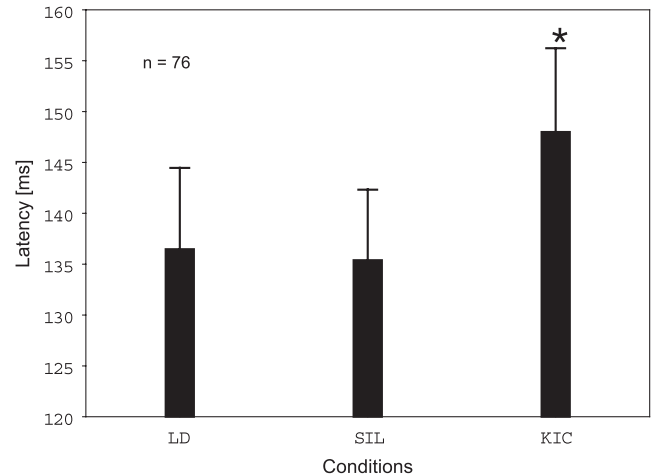


FIG. 8. Mean neuronal response onset latency values for LDs, SILs and KICs. Bars indicate means, whiskers show 0.95 confidence intervals. The onset latency was longer for the KICs than for those measured in the other two conditions.  $*P < 0.5$ , compared with LD and SIL.

- (i) The neurones in the IT cortex are responsive to KICs.
- (ii) The neuronal response onset latencies for KICs are longer than those for shapes with real contours (LDs and SILs).
- (iii) The IT cortical cells exhibit clear shape selectivity for KIC stimuli.
- (iv) The shape selectivity of the IT cortical neurones differs from that for LDs or SILs, but the degree and similarity of selectivity were the closest between KICs and SILs.

(i) The present study complements the recently published one by Sary *et al.* (2007), in which ICs based on abutting-line gratings were used as visual stimuli. We found that in contrast to the previous study, in which the abutting-line stimuli elicited much smaller responses than did the stimuli with real contours, KICs proved to be very effective stimuli in the present study; the mean response level to KICs being somewhat higher than that for real contours. It should be noted, however, that in this study achromatic line drawing shapes were used, and it is known that IT cortical cells prefer complex chromatic shapes (Komatsu *et al.*, 1992; Komatsu & Ideura, 1993; Tamura & Tanaka, 2001; Edwards *et al.*, 2003) and simple line drawings may not trigger maximum responses, even when the inducing pacmen are present. On the other hand, the 'hunting stimuli' used to isolate the cells were achromatic LDs and thus one may expect that response levels would have been biased towards these stimulus type. Further, it has been reported that IT cortical cells might be insensitive to the removal of colours from the stimuli (Tompa *et al.*, 2005) and that response levels are not necessarily associated with the presence or absence of colours.

KIC stimuli elicited much higher responses than the CTR stimuli, suggesting that the responses to the KICs are due not simply to the inducers (the pacmen) but also to the KICs inducing the shape from the background, even if real contours are absent. This is in line with those results where variants of the pacmen did not change P1 waves in a visual evoked potential study using Kanizsa-type stimuli (Brodeur *et al.*, 2006), although the P1 wave is known to be very sensitive to the physical features of the stimuli (Jeffreys, 1996).

(ii) The response latencies to the KICs were longer than those to the stimuli with real contours, LDs or SILs. Our latency values fit nicely with the latency values obtained for ICs, which range from 130 to 180 ms (Kruggel *et al.*, 2001; Botterger *et al.*, 2002), associated with the lateral occipital cortex (Murray *et al.*, 2004). Moreover, the use of KIC

stimuli has revealed that the most prominent evoked responses occur at only ~150 ms over the anterolateral occipital cortex (Halgren *et al.*, 2003), which is considered to have a similar function in humans as the IT cortex in monkeys (Grill-Spector *et al.*, 1998, 2001; Kourtzi & Kanwisher, 2000). Processing of ICs is delayed in the early parts of the visual pathway as well. V1 neurones are responsive to the orientation of ICs defined by abutting gratings and KICs (Lee & Nguyen, 2001; Ramsden *et al.*, 2001), but the responses emerge later than those for real contours. This delay and the fact that the responses in V1 emerge 30 ms later than those in V2 suggest possible intercortical interactions during processing of ICs. [Some findings suggest that when abutting-line gratings are used as stimuli the orientation maps in V1 and V2 depend critically on the spatial frequency of the stimuli (Zhan & Baker, 2008), and IC sizes in the interval 5–10° do not elicit significant responses over V1/V2 (Mendola *et al.*, 1999; Murray *et al.*, 2002)].

(iii) Our data indicate that neuronal responses from the IT cortex to KICs can be used to construct tuning curves with a significant slope while the same curves for CTR stimuli are essentially flat. This shows that IT cortical neurones have a stimulus preference and can reliably discriminate between stimuli even in the absence of real contours. Human studies suggested the contribution of the anterolateral occipital cortex in illusory shape perception (Kourtzi & Kanwisher, 2001; Kruggel *et al.*, 2001; Pegna *et al.*, 2002; Halgren *et al.*, 2003). Here we provide direct evidence that the monkey IT cortex can code unambiguously the presence of illusory contours in the stimuli. In this respect, these findings mirror the results of the previous study (Sary *et al.*, 2007) and suggest that IT cells with shape-selective responses to KICs (and to ICs in general) might participate in the perception of IC-defined shapes where no real contour information is available.

(iv) In our previous study we found that the selectivity of IT cells was different for coloured stimuli and ICs, but IC selectivity did not differ from that of SILs (Sary *et al.*, 2007). The present study demonstrated that shape selectivity for KICs was different from those for the SILs and LDs. This is somewhat surprising as KICs usually give the impression of a floating surface which lacks internal visual surface information, in a manner similar to SILs. There are different possible explanations for this. On the one hand, ICs contain much more ambiguity than real contours or SILs and thus are harder to perceive, which is also reflected in longer reaction times in psychophysical studies (Ringach & Shapley, 1996; Rajimehr *et al.*, 2003; Brodeur *et al.*, 2008) and longer neuronal onset latencies in IT cortex (Sary *et al.*, 2007). On the other hand, IT cells might react to forms defined by different visual cues similarly but they are not invariant to depth segmentation, which is a common phenomenon associated with KICs. IT cortical responses depend not only on the presented shape but also on the border ownership polarity of the contours (Baylis & Driver, 2001). The presence of the additional depth information in the KICs and the absence of the same in SILs might explain the differences in the tuning curves we observed.

Shape selectivity of IT cortical neurones is a well-studied issue (Sary *et al.*, 1993, 2007; Vogels & Biederman, 2002; Kovacs *et al.*, 2003; Tompa *et al.*, 2005). This selectivity may underlie the perceptual invariances of object recognition (Sary *et al.*, 1993; Rolls, 2000; Tanaka *et al.*, 2001; Vogels & Biederman, 2002; Kovacs *et al.*, 2003; Tompa *et al.*, 2005). We think that the relation of shape preferences of IT cortical neurones for the KICs and the real contour-defined shapes might form the basis for the perceptual effects observed for real and illusory contours (Smith & Over, 1979; Vogels & Orban, 1987; Paradiso *et al.*, 1989; Berkley *et al.*, 1994; Dresch & Bonnet, 1995; Brodeur *et al.*, 2008). Our results confirm the role of IT cortex in

visual shape perception and generalize the IT cortical function in object and shape coding into the IC domain.

Two possible mechanisms of processing contours or surfaces physically not present (especially in those areas where the receptive fields of the neurons are smaller than the distance between the inducers) are the lateral connections and the feedback flow of information. In the first case, cells which have line endings or inducers interpretable as line endings in their receptive fields can facilitate other cells having similar orientation selectivity and receptive fields situated between the facilitators, inducing thereby the percept of a dim line (Rockland *et al.*, 1982; Polat *et al.*, 1998; Kapadia *et al.*, 1999; Kasamatsu *et al.*, 2001; Bauer & Heinze, 2002; Li *et al.*, 2006). In the second case, cells in higher order visual areas having large enough receptive fields to contain two or more inducers can facilitate backwards those cells, which would participate in the representation of the shape (surface or contours) formed by the inducers (Bullier & Henry, 1979; Givre *et al.*, 1994). Of course the two strategies are not mutually exclusive; they can even work together in shaping the appropriate percept (Oliva & Schyns, 1997).

These strategies are paralleled by the scene-segmentation strategies of edge detection vs. surface representation. An effective conducive to the recognition of objects, especially if they are occluded, is the exploration of their borders, i.e. a kind of edge detection. Indeed, it seems that an important feature of visual neurones is the representation of oriented lines. At the same time it is at least equally important to have information about whose border the given line is, namely the border ownership. The borders are borders of surfaces, so one has to identify the surfaces to assign the borders. Which strategy dominates in the recognition of illusory contours and, generally, of objects? Is one of them dominant or do they act together in the process of recognition?

An empirical way to find the strategy can be the analysis of the response latencies and the comparison of the responses of individual neurons given to the illusory contours and to the illusory vs. the real contours, in a given area or at different levels of the presumed hierarchy of the visual system. The response latency of the neurons recorded by us is longer in the case of the illusory contours (see also Sary *et al.*, 2007) than to the real ones and to the silhouettes representing the surfaces. This means additional processing, i.e. those higher order visual areas do not rely simply on the feedforward information flow when identifying shapes. More cells had similar selectivity for the KIC and SIL condition than in the case of the KIC vs. LD comparison (see Table 1), indicating that the processing of illusory contour-defined shapes shares more features with surface processing than with contour or edge processing. A similar conclusion can be drawn from the case of the abutting grating-defined ICs (Sary *et al.*, 2007), where even the selectivity for the IC and SIL conditions were similar. We found, however, cells having similar contour selectivity for illusory and real contours, meaning that the strategy of edge detection is present as well in the system. (There were also cells with differing selectivity for all three conditions. They may contribute to a third strategy.) Given that at the behavioural level there is a level of invariance for the shapes defined by different cues, we have to conclude that the different neural strategies will indeed yield the same or similar behavioural outcomes; this is analogous to the situation in which we can chose different means of transportation when travelling to the same destination. The longer response latency in early visual areas for ICs as compared to real contours (Lee & Nguyen, 2001) suggests a role for feedback connections in processing of subjective contours. A good candidate for the origin of this feedback information would be the global shape processor IT. Indeed,

a number of studies has shown that these higher order visual areas (in both humans and monkeys) have substantial roles in the IC processing (Imber *et al.*, 2005; Seghier & Vuilleumier, 2006; Montaser-Kouhsari *et al.*, 2007). However, neuronal response latencies in the IT are still longer than those for the real contours, and this finding is consistent with our previous results (Sary *et al.*, 2007). This fact suggests that IT is not the (sole) provider of this information but seems to need further cortical sources to provide the information for the visual system. From where then emerges this information?

The longer response latency is in line with the findings that some illusions, e.g. the surface-linked brightness illusion, seem to rely on 'tacit inference' which of course requires the contribution of higher order areas (Purves *et al.*, 1999; Paradiso, 2000; Hung *et al.*, 2007). Some even argue that in order to perceive these phenomena the visual system needs learning (Gilbert & Sigman, 2007; Li *et al.*, 2008). In the case of illusory contours it is strengthened by the required grouping effect of the inducers (Elder & Zucker, 1998) and by the illusion that the surface of the illusory object is perceived as brighter than the surrounding.

Based on the above-presented evidence, one can conclude that the higher order areas play a role in the processing of the shapes defined by illusory contours. They can be the source of feedback information going to early visual areas (which, in turn, are needed for the detailed representation of the figures; Lee, 2002; Pillow & Rubin, 2002) but, at the same time, they seem to need more computation than for the processing of shapes defined in a more unambiguous way.

## Acknowledgements

This work was supported by grant K68594 OTKA/Hungary. The authors are grateful to G. Dósa and P. Liszli for technical assistance, to K. Hermann for maintaining the laboratory equipment and to A. Arnold for taking care of the laboratory animals.

## Abbreviations

CTRs, control stimuli; ICs, illusory contours; IT, inferior temporal (cortex); KICs, Kanizsa-type ICs; LDs, line drawings; PSTH, peristimulus time histogram; SILs, silhouettes.

## References

- Bauer, R. & Heinze, S. (2002) Contour integration in striate cortex. Classic cell responses or cooperative selection? *Exp. Brain Res.*, **147**, 145–152.
- Baylis, G.C. & Driver, J. (2001) Shape-coding in IT cells generalizes over contrast and mirror reversal, but not figure-ground reversal. *Nat. Neurosci.*, **4**, 937–942.
- Berkley, M.A., DeBruyn, B. & Orban, G. (1994) Illusory, motion, and luminance-defined contours interact in the human visual system. *Vision Res.*, **34**, 209–216.
- Booth, M.C. & Rolls, E.T. (1998) View-invariant representations of familiar objects by neurons in the inferior temporal visual cortex. *Cereb. Cortex*, **8**, 510–523.
- Bottger, D., Herrmann, C.S. & von Cramon, D.Y. (2002) Amplitude differences of evoked alpha and gamma oscillations in two different age groups. *Int. J. Psychophysiol.*, **45**, 245–251.
- Brodeur, M., Lepore, F. & DeBruille, J.B. (2006) The effect of interpolation and perceptual difficulty on the visual potentials evoked by illusory figures. *Brain Res.*, **1068**, 143–150.
- Brodeur, M., Lepore, F., Lepage, M., Bacon, B.A., Jemel, B. & DeBruille, J.B. (2008) Alternative mode of presentation of Kanizsa figures sheds new light on the chronometry of the mechanisms underlying the perception of illusory figures. *Neuropsychologia*, **46**, 554–566.
- Bullier, J. & Henry, G.H. (1979) Neural path taken by afferent streams in striate cortex of the cat. *J. Neurophysiol.*, **42**, 1264–1270.

- Dean, P. (1976) Effects of inferotemporal lesions on the behavior of monkeys. *Psychol. Bull.*, **83**, 41–71.
- DiCarlo, J.J. & Maunsell, J.H. (2000) Form representation in monkey inferotemporal cortex is virtually unaltered by free viewing. *Nat. Neurosci.*, **3**, 814–821.
- Dresp, B. & Bonnet, C. (1995) Subthreshold summation with illusory contours. *Vision Res.*, **35**, 1071–1078.
- Edwards, R., Xiao, D., Keysers, C., Foldiak, P. & Perrett, D. (2003) Color sensitivity of cells responsive to complex stimuli in the temporal cortex. *J. Neurophysiol.*, **90**, 1245–1256.
- Elder, J.H. & Zucker, S.W. (1998) Evidence for boundary-specific grouping. *Vision Res.*, **38**, 143–152.
- Gilbert, C.D. & Sigman, M. (2007) Brain states: top-down influences in sensory processing. *Neuron*, **54**, 677–696.
- Givre, S.J., Schroeder, C.E. & Arezzo, J.C. (1994) Contribution of extrastriate area V4 to the surface-recorded flash VEP in the awake macaque. *Vision Res.*, **34**, 415–428.
- Grill-Spector, K., Kushnir, T., Edelman, S., Itzhak, Y. & Malach, R. (1998) Cue-invariant activation in object-related areas of the human occipital lobe. *Neuron*, **21**, 191–202.
- Grill-Spector, K., Kourtzi, Z. & Kanwisher, N. (2001) The lateral occipital complex and its role in object recognition. *Vision Res.*, **41**, 1409–1422.
- Grosf, D.H., Shapley, R.M. & Hawken, M.J. (1993) Macaque V1 neurons can signal 'illusory' contours. *Nature*, **365**, 550–552.
- Halgren, E., Mendola, J., Chong, C.D. & Dale, A.M. (2003) Cortical activation to illusory shapes as measured with magnetoencephalography. *Neuroimage*, **18**, 1001–1009.
- Hasselmo, M.E., Rolls, E.T., Baylis, G.C. & Nalwa, V. (1989) Object-centered encoding by face-selective neurons in the cortex in the superior temporal sulcus of the monkey. *Exp. Brain Res.*, **75**, 417–429.
- von der Heydt, R., Peterhans, E. & Baumgartner, G. (1984) Illusory contours and cortical neuron responses. *Science*, **224**, 1260–1262.
- Hung, C.P., Ramsden, B.M. & Roe, A.W. (2007) A functional circuitry for edge-induced brightness perception. *Nat. Neurosci.*, **10**, 1185–1190.
- Huxlin, K.R., Saunders, R.C., Marchionini, D., Pham, H.A. & Merigan, W.H. (2000) Perceptual deficits after lesions of inferotemporal cortex in macaques. *Cereb. Cortex*, **10**, 671–683.
- Imber, M.L., Shapley, R.M. & Rubin, N. (2005) Differences in real and illusory shape perception revealed by backward masking. *Vision Res.*, **45**, 91–102.
- Jeffreys, D.A. (1996) Simple methods of identifying the independently generated components of scalp-recorded responses evoked by stationary patterns. *Exp. Brain Res.*, **111**, 100–112.
- Judge, S.J., Richmond, B.J. & Chu, F.C. (1980) Implantation of magnetic search coils for measurement of eye position: an improved method. *Vision Res.*, **20**, 535–538.
- Kanizsa, G. (1976) Subjective contours. *Sci. Am.*, **234**, 48–52.
- Kapadia, M.K., Westheimer, G. & Gilbert, C.D. (1999) Dynamics of spatial summation in primary visual cortex of alert monkeys. *Proc. Natl Acad. Sci. USA*, **96**, 12073–12078.
- Kasamatsu, T., Polat, U., Pettet, M.W. & Norcia, A.M. (2001) Colinear facilitation promotes reliability of single-cell responses in cat striate cortex. *Exp. Brain Res.*, **138**, 163–172.
- Komatsu, H. & Ideura, Y. (1993) Relationships between color, shape, and pattern selectivities of neurons in the inferior temporal cortex of the monkey. *J. Neurophysiol.*, **70**, 677–694.
- Komatsu, H., Ideura, Y., Kaji, S. & Yamane, S. (1992) Color selectivity of neurons in the inferior temporal cortex of the awake macaque monkey. *J. Neurosci.*, **12**, 408–424.
- Kourtzi, Z. & Kanwisher, N. (2000) Cortical regions involved in perceiving object shape. *J. Neurosci.*, **20**, 3310–3318.
- Kourtzi, Z. & Kanwisher, N. (2001) Representation of perceived object shape by the human lateral occipital complex. *Science*, **293**, 1506–1509.
- Kovacs, G., Sary, G., Koteles, K., Chadaide, Z., Tompa, T., Vogels, R. & Benedek, G. (2003) Effects of surface cues on macaque inferior temporal cortical responses. *Cereb. Cortex*, **13**, 178–188.
- Kruggel, F., Herrmann, C.S., Wiggins, C.J. & von Cramon, D.Y. (2001) Hemodynamic and electroencephalographic responses to illusory figures: recording of the evoked potentials during functional MRI. *Neuroimage*, **14**, 1327–1336.
- Larsson, J., Amunts, K., Gulyas, B., Malikovics, A., Zilles, K. & Roland, P.E. (1999) Neuronal correlates of real and illusory contour perception: functional anatomy with PET. *Eur. J. Neurosci.*, **11**, 4024–4036.
- Lee, T.S. (2002) The nature of illusory contour computation. *Neuron*, **33**, 667–668.

- Lee, T.S. & Nguyen, M. (2001) Dynamics of subjective contour formation in the early visual cortex. *Proc. Natl Acad. Sci. USA*, **98**, 1907–1911.
- Legendy, C.R. & Salzman, M. (1985) Bursts and recurrences of bursts in the spike trains of spontaneously active striate cortex neurons. *J. Neurophysiol.*, **53**, 926–939.
- Li, W., Piech, V. & Gilbert, C.D. (2006) Contour saliency in primary visual cortex. *Neuron*, **50**, 951–962.
- Li, W., Piech, V. & Gilbert, C.D. (2008) Learning to link visual contours. *Neuron*, **57**, 442–451.
- Logothetis, N.K. & Sheinberg, D.L. (1996) Visual object recognition. *Annu. Rev. Neurosci.*, **19**, 577–621.
- Logothetis, N.K., Pauls, J. & Poggio, T. (1995) Shape representation in the inferior temporal cortex of monkeys. *Curr. Biol.*, **5**, 552–563.
- Maertens, M. & Pollmann, S. (2005) fMRI reveals a common neural substrate of illusory and real contours in V1 after perceptual learning. *J. Cogn. Neurosci.*, **17**, 1553–1564.
- Mendola, J.D., Dale, A.M., Fischl, B., Liu, A.K. & Tootell, R.B. (1999) The representation of illusory and real contours in human cortical visual areas revealed by functional magnetic resonance imaging. *J. Neurosci.*, **19**, 8560–8572.
- Merigan, W.H. (1996) Basic visual capacities and shape discrimination after lesions of extrastriate area V4 in macaques. *Vis. Neurosci.*, **13**, 51–60.
- Montaser-Kouhsari, L., Landy, M.S., Heeger, D.J. & Larsson, J. (2007) Orientation-selective adaptation to illusory contours in human visual cortex. *J. Neurosci.*, **27**, 2186–2195.
- Murray, M.M., Wylie, G.R., Higgins, B.A., Javitt, D.C., Schroeder, C.E. & Foxe, J.J. (2002) The spatiotemporal dynamics of illusory contour processing: combined high-density electrical mapping, source analysis, and functional magnetic resonance imaging. *J. Neurosci.*, **22**, 5055–5073.
- Murray, M.M., Foxe, D.M., Javitt, D.C. & Foxe, J.J. (2004) Setting boundaries: brain dynamics of modal and amodal illusory shape completion in humans. *J. Neurosci.*, **24**, 6898–6903.
- Oliva, A. & Schyns, P.G. (1997) Coarse blobs or fine edges? Evidence that information diagnosticity changes the perception of complex visual stimuli. *Cognit. Psychol.*, **34**, 72–107.
- Paradiso, M.A. (2000) Visual neuroscience: illuminating the dark corners. *Curr. Biol.*, **10**, R15–R18.
- Paradiso, M.A., Shimojo, S. & Nakayama, K. (1989) Subjective contours, tilt aftereffects, and visual cortical organization. *Vision Res.*, **29**, 1205–1213.
- Paxinos, G., Huang, F.X. & Toga, A.W. (1999) *The Rhesus Monkey Brain in Stereotaxic Coordinates*. Academic Press, New York.
- Pegna, A.J., Khateb, A., Murray, M.M., Landis, T. & Michel, C.M. (2002) Neural processing of illusory and real contours revealed by high-density ERP mapping. *Neuroreport*, **13**, 965–968.
- Peterhans, E. & von der Heydt, R. (1991) Subjective contours – bridging the gap between psychophysics and physiology. *Trends Neurosci.*, **14**, 112–119.
- Pillow, J. & Rubin, N. (2002) Perceptual completion across the vertical meridian and the role of early visual cortex. *Neuron*, **33**, 805–813.
- Polat, U., Mizobe, K., Pettet, M.W., Kasamatsu, T. & Norcia, A.M. (1998) Collinear stimuli regulate visual responses depending on cell's contrast threshold. *Nature*, **391**, 580–584.
- Purves, D., Shimp, A. & Lotto, R.B. (1999) An empirical explanation of the cornsweet effect. *J. Neurosci.*, **19**, 8542–8551.
- Rajimehr, R., Montaser-Kouhsari, L. & Afraz, S.R. (2003) Orientation-selective adaptation to crowded illusory lines. *Perception*, **32**, 1199–1210.
- Ramachandran, V.S. (1987) Interaction between colour and motion in human vision. *Nature*, **328**, 645–647.
- Ramsden, B.M., Hung, C.P. & Roe, A.W. (2001) Real and illusory contour processing in area V1 of the primate: a cortical balancing act. *Cereb. Cortex*, **11**, 648–665.
- Ringach, D.L. & Shapley, R. (1996) Spatial and temporal properties of illusory contours and amodal boundary completion. *Vision Res.*, **36**, 3037–3050.
- Rockland, K.S., Lund, J.S. & Humphrey, A.L. (1982) Anatomical binding of intrinsic connections in striate cortex of tree shrews (*Tupaia glis*). *J. Comp. Neurol.*, **209**, 41–58.
- Rolls, E.T. (2000) Functions of the primate temporal lobe cortical visual areas in invariant visual object and face recognition. *Neuron*, **27**, 205–218.
- Rolls, E.T. & Baylis, G.C. (1986) Size and contrast have only small effects on the responses to faces of neurons in the cortex of the superior temporal sulcus of the monkey. *Exp. Brain Res.*, **65**, 38–48.
- Sary, G., Vogels, R. & Orban, G.A. (1993) Cue-invariant shape selectivity of macaque inferior temporal neurons. *Science*, **260**, 995–997.
- Sary, G., Chadaide, Z., Tompa, T., Kovacs, G., Koteles, K., Boda, K., Raduly, L. & Benedek, G. (2004) Relationship between stimulus complexity and neuronal activity in the inferotemporal cortex of the macaque monkey. *Cogn. Brain Res.*, **22**, 1–12.
- Sary, G., Koteles, K., Chadaide, Z., Tompa, T. & Benedek, G. (2006) Task-related modulation in the monkey inferotemporal cortex. *Brain Res.*, **1121**, 76–82.
- Sary, G., Chadaide, Z., Tompa, T., Koteles, K., Kovacs, G. & Benedek, G. (2007) Illusory shape representation in the monkey inferior temporal cortex. *Eur. J. Neurosci.*, **25**, 2558–2564.
- Seghier, M.L. & Vuilleumier, P. (2006) Functional neuroimaging findings on the human perception of illusory contours. *Neurosci. Biobehav. Rev.*, **30**, 595–612.
- Sheth, B.R., Sharma, J., Rao, S.C. & Sur, M. (1996) Orientation maps of subjective contours in visual cortex 18. *Science*, **274**, 2110–2115.
- Smith, A.T. & Over, R. (1979) Motion aftereffect with subjective contours. *Percept. Psychophys.*, **25**, 95–98.
- Sugase, Y., Yamane, S., Ueno, S. & Kawano, K. (1999) Global and fine information coded by single neurons in the temporal visual cortex. *Nature*, **400**, 869–873.
- Tamura, H. & Tanaka, K. (2001) Visual response properties of cells in the ventral and dorsal parts of the macaque inferotemporal cortex. *Cereb. Cortex*, **11**, 384–399.
- Tanaka, K. (1992) Inferotemporal cortex and higher visual functions. *Curr. Opin. Neurobiol.*, **2**, 502–505.
- Tanaka, K. (1996) Inferotemporal cortex and object vision. *Annu. Rev. Neurosci.*, **19**, 109–139.
- Tanaka, H., Uka, T., Yoshiyama, K., Kato, M. & Fujita, I. (2001) Processing of shape defined by disparity in monkey inferior temporal cortex. *J. Neurophysiol.*, **85**, 735–744.
- Tompa, T., Sary, G., Chadaide, Z., Koteles, K., Kovacs, G. & Benedek, G. (2005) Achromatic shape processing in the inferotemporal cortex of the macaque. *Neuroreport*, **16**, 57–61.
- Tovee, M.J., Rolls, E.T. & Azzopardi, P. (1994) Translation invariance in the responses to faces of single neurons in the temporal visual cortical areas of the alert macaque. *J. Neurophysiol.*, **72**, 1049–1060.
- Vogels, R. (1999) Categorization of complex visual images by rhesus monkeys. Part I: behavioural study. *Eur. J. Neurosci.*, **11**, 1223–1238.
- Vogels, R. & Biederman, I. (2002) Effects of illumination intensity and direction on object coding in macaque inferior temporal cortex. *Cereb. Cortex*, **12**, 756–766.
- Vogels, R. & Orban, G.A. (1987) Illusory contour orientation discrimination. *Vision Res.*, **27**, 453–467.
- Wallis, G. & Rolls, E.T. (1997) Invariant face and object recognition in the visual system. *Prog. Neurobiol.*, **51**, 167–194.
- Zhan, C.A. & Baker, C.L. Jr (2008) Critical spatial frequencies for illusory contour processing in early visual cortex. *Cereb. Cortex*, **18**, 1029–1041.